Chemistry & Biology, Vol. 10, 411–417, May, 2003, ©2003 Elsevier Science Ltd. All rights reserved. DOI 10.1016/S1074-5521(03)00094-2

Rational Design and Molecular Diversity for the Construction of Anti-α-Bungarotoxin Antidotes with High Affinity and In Vivo Efficiency

Luisa Lozzi, Barbara Lelli, Ylenia Runci, Silvia Scali, Andrea Bernini, Chiara Falciani, Alessandro Pini, Neri Niccolai, Paolo Neri, and Luisa Bracci*
Department of Molecular Biology
University of Siena
via Fiorentina 1
I-53100 Siena
Italy

Summary

The structure of peptide p6.7, a mimotope of the nicotinic receptor ligand site that binds α-bungarotoxin and neutralizes its toxicity, was compared to that of the acetylcholine binding protein. The central loop of p6.7, when complexed with α-bungarotoxin, fits the structure of the *a*cetylcholine *b*inding *p*rotein (AChBP) ligand site, whereas peptide terminal residues seem to be less involved in toxin binding. The minimal binding sequence of p6.7 was confirmed experimentally by synthesis of progressively deleted peptides. Affinity maturation was then achieved by random addition of residues flanking the minimal binding sequence and by selection of new α-bungarotoxin binding peptides on the basis of their dissociation kinetic rate. The tetra-branched forms of the resulting high-affinity peptides were effective as antidotes in vivo at a significantly lower dose than the tetra-branched lead peptide.

Introduction

New drugs can be designed rationally using protein structural information and molecular modeling. Molecular diversity can be constructed by using combinatorial libraries of potentially bioactive molecules. These can be used to empirically "fish" active ligands from a large number of structural combinations. Structure-based molecular design and construction of molecular diversity are not mutually exclusive, but can be combined to develop specifically targeted drugs.

Peptide libraries, expressed on phages or obtained by solid-phase synthesis [1, 2], can be used to select specific sequences, named mimotopes, which, although different from native sequences, can mimic structural and functional features of domains of proteins [3, 4]. Mimotopes can reproduce protein recognition surfaces, like those involved in antigen-antibody [5, 6] or ligand-receptor recognition [7, 8]. This property gives them useful diagnostic and therapeutic applications.

In a previous paper we described the production of peptide mimotopes of the α-bungarotoxin (α-bgt) binding site of nicotinic acetylcholine receptors (nAchR) [9]. Nicotinic receptors are ligand-gated ion channels composed of five homologous, membrane-spanning subunits (see [10] for a recent review). Postsynaptic snake neurotoxins, like α-bgt, bind with high affinity to nAchR and have been extremely useful in the location of nAchR ligand sites.

The three-dimensional structure of nicotinic receptor subunits has not yet been solved. However, a sequence of α subunit amino-terminal domain, which contains the highly conserved cysteine residues 192 and 193 (sequence numbering of α1 subunit from *Torpedo* electric organs), was determined as containing at least part of the nAchR ligand binding site [10, 11]. Synthetic peptides reproducing this sequence of muscle α1 and neuronal α7 nAchR subunits still bind α-bgt, albeit with much lower affinity [12–14].

Due to lack of information on three-dimensional structure, mimotopes of the receptor ligand site have essentially been obtained by two different approaches. An α-bgt binding peptide mimotope, LLPep (with the sequence MRYYESSLKSYPD), was selected from a random phage library [15] and optimized on the basis of the peptide-toxin NMR structure to obtain the high-affinity peptide HAPep (WRYYESSLEPYPD) [16]. In our previous study [9], another α-bgt binding peptide mimotope (p6.7, with the sequence HRYYESSLEPWYPD) of higher affinity than LLPep was selected by systematic analysis of a synthetic peptide combinatorial library. This was designed on the basis of amino acid sequence comparison around C192 and C193 of α-bgt binding subunits from different nAchR. Different α-bgt binding peptides with higher binding capacity than those reproducing native receptor sequences were selected from the peptide combinatorial library. Among these, p6.7 inhibited α-bgt binding to muscle and neuronal receptors with a half-maximal inhibition constant (IC_{50}) at least 50 times lower than that of peptides reproducing native sequences. Moreover, a tetra-branched form of p6.7 can protect mice against the lethal effect of the toxin [17].

The three-dimensional structures of the complexes of α-bgt and p6.7 [18], LLPep [19], and HAPep [20, 21] respectively were solved and their affinity, and binding kinetic constants were compared and analyzed with respect to their NMR structure [22]. A determinant contribution for understanding the three-dimensional organization of nAchR ligand sites came from the crystal structure of the acetylcholine binding protein (AChBP) [23, 24]. AChBP is a soluble homopentameric transmitter receptor, structurally and functionally related to the amino-terminal domain of nAchR α subunits containing the ligand site, and binds several nicotinic ligands, including α-bgt. The sequence similarity of AChBP and nAchR α subunits makes it possible to locate AChBP ligand sites on loops at interfaces between each subunit. The structure of AChBP homopentamer and its ligand binding sites is presently the most reliable model for studying nicotinic receptor binding sites, and it has already been compared with the structures of the mimotope peptide HAPep [21] and of two cognate peptides, reproducing the 178–196 and the 182–202 sequence

*Correspondence: braccil@unisi.it

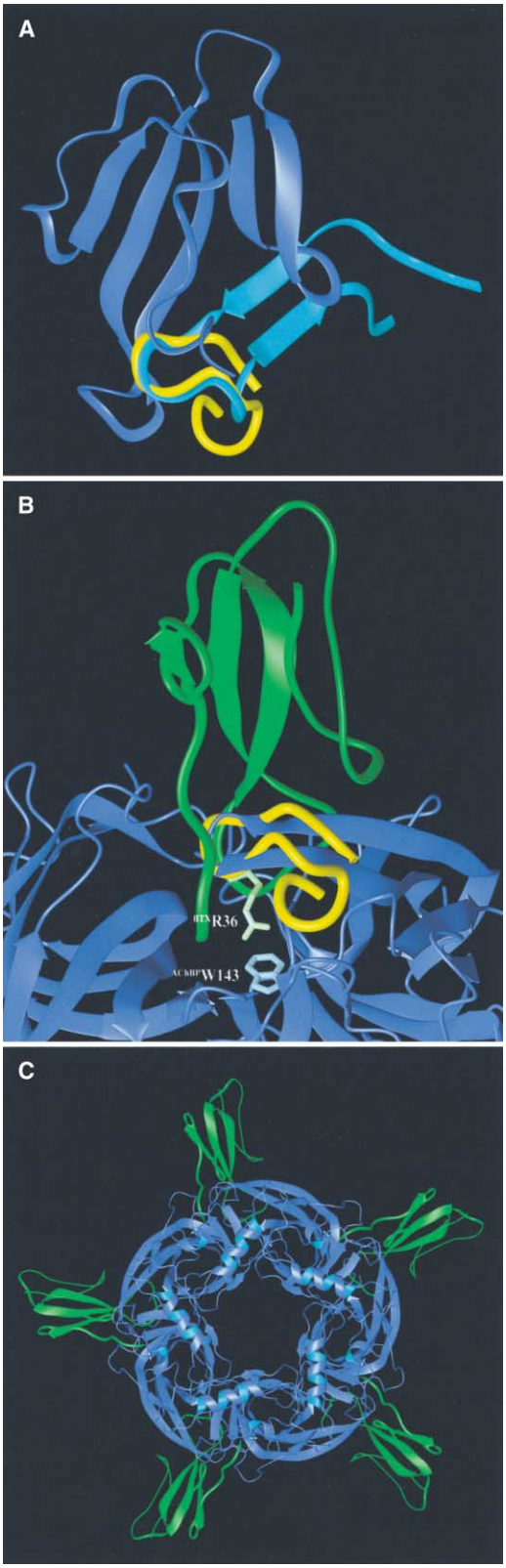

Figure 1. Comparison of p6.7 with Structural Models of the Nicotinic Receptor Binding Site

(A) Structural superposition of p6.7 from α-bgt/p6.7 complex (PDB ID 1JBD) on α1 (182-202)-α-bgt complex (PDB ID 1L4W). Structures of the toxin and α1 peptide in bound form are colored blue and cyan, respectively; p6.7 is colored yellow.

(B) Structural superposition of p6.7-α-bgt complex (PDB ID 1JBD) on putative ligand binding loop of AChBP (PDB ID 1I9B): close view of the backbone fitting result for residues 3–10 of p6.7 on residues 184–191 of AchBP. Toxin R36 is stacking onto AChBP W143. Structures of toxin and peptide are colored green and yellow, respectively; AChBP is colored blue.

(C) Toxin-AChBP complex as viewed down the oligomer 5-fold axis.

Table 1. p6.7 Sequence Alignment with α1 Peptide and the Putative Binding Loop of AchBP

Sequence	PDB ID	Alignment
		1 14
p6.7	1JBD	HRYYESSLEPWYPD
α1	1L4W	RGWKHWVYYTCCPDTPYLDIT
		182 202
		1 14
p6.7	1JBD	HRYYESSLEPWYPD
AChBP	1I9B	TQKKNSVTYSCCPEA-YEDVE
		177 196

Stretches showing the best three-dimensional superposition are highlighted in bold, with a calculated rmsd of 1.50 and 1.32 Å for α1 and AChBP, respectively.

of the neuronal α7 [25] and muscle α1 [26] subunit, respectively.

In the present study, we compared the structure of the peptide mimotope p6.7 with that of homologous sequences from AChBP and the α1 peptide described in [26]. Structural information was used in association with kinetic binding data, obtained by surface plasmon resonance (SPR) on progressively deleted p6.7. This provided information on the essential toxin binding region of p6.7. Affinity maturation of the peptide was then obtained by random addition of residues flanking the minimal binding sequence, followed by empirical selection of new binding sequences on the basis of their dissociation kinetic rate constant (k_{off}).

A tetra-branched dendrimer of a high-affinity peptide obtained by this procedure is more effective for in vivo neutralization of α-bgt toxicity than the tetra-branched p6.7, and more active than any other analogous peptide mimotope described so far.

Results and Discussion

Comparison of p6.7 with Structural Models of the Nicotinic Receptor Binding Site

The three-dimensional structure of α-bgt-bound p6.7 (PDB ID 1JBD) [18] was compared to that of a 21-mer peptide reproducing the 182–202 sequence of the α1 subunit of nicotinic receptor from *Torpedo* electric organs (RGWKHWVYYTCCPDTPYLDIT, PDB ID 1L4W) [26] when bound to the same toxin, to obtain a good rmsd (≤1.50 Å) using the maximum number of residues (Figure 1A). The best superposition was found for residues 189–196 and 3–10 of α1 peptide and p6.7 respectively, giving an rmsd of 1.50 for backbone atoms (Table 1). The region showing good structural agreement was that of the central loop carrying tyrosine 190 and cysteines 192 and 193 of α1 peptide. The turn region of peptide p6.7 showed a high structural similarity to that

of the native sequence when bound to α-bgt. In both cases, the loops matched the key region of interaction.

The same procedure was repeated to overlay the structure of α-bgt-bound p6.7 on the homologous sequence of the loop of AChBP from *Lymnaea stagnalis* [23, 24], which contains the putative AChBP ligand site (PDB ID 1I9B) (Figures 1B and 1C). A backbone rmsd of 1.32 Å was obtained for stretches 3–10 and 184–191 of the peptide and protein respectively (Table 1). Again, there is a very good three-dimensional structural agreement between the central turns of p6.7 and of the native protein.

Superposition of the peptide of the α-bgt/p6.7 complex on the loop of AChBP gave another interesting result. Assuming that peptide and protein loop interact in the same way, a hypothetical model of the α-bgt/AChBP complex can be obtained. Superposition showed that toxin loops 1 and 2 and the C terminus region fit the AChBP surface, with no Van der Waals violations greater than 0.60 Å for backbone atoms, but three of approximately 1 Å. A model of interaction between α-bgt and nicotinic receptors can therefore be obtained (Figures 1B and 1C). The model was also compared to that previously proposed in [21] between the same AChBP and α-bgt/HAPep complex (PDB ID 1HC9), which we reconstructed from the PDB structure files, following the fitting procedure reported on the paper. Our model confirms the geometry of the complex proposed in [21], which differs only for the presence of more backbone clashes (six Van der Waals violations greater than 0.60 Å, three greater than 1 Å, and one greater than 2 Å).

In the AChBP crystal structure [24], an acetylcholine binding site was identified, indeed, by the presence of a N-2-hydroxyethylpiperazine-N′-2-ethanesulphonic acid (HEPES) positively charged buffer molecule situated in a cleft underneath the aforementioned loop and making a cation-π interaction with W143, as expected for nicotinic agonists [27, 28]. Such residue is also conserved in *Torpedo* nAchR α subunit sequence (W149). Interestingly, in our model the HEPES molecule is replaced by α-bgt R36 guanidinium group, which makes a cation-π interaction with the same W143 (see Figure 1B), suggesting a general mechanisms for receptor binding by acetylcholine mimics. Such observation confirms the findings reported in [21] and those recently reported in [26] and [29], based on a combination of homology modeling and NMR structure reconstruction of the three-dimensional structure of AchR extracellular domain in complex with α-bgt and α-cobratoxin, respectively. The authors proposed this cation-π interaction as general mechanisms for receptor binding by acetylcholine mimics.

Definition of the Minimal Essential Residues for p6.7-α-bgt Binding

Structural comparison of the complexes formed by α-bgt with p6.7, and with structures that can be taken as models of the nicotinic receptor ligand site, indicated that the central loop of p6.7 is the main interacting structure, whereas peptide terminal residues seem to be less involved in toxin binding.

In order to confirm critical residues for α-bgt binding, different peptides were synthesized reproducing the 14-mer sequence H_1RYYESSLEPWYPD$_{14}$, progressively shortened at the N- and C termini. Peptides were then analyzed for α-bgt binding by injecting them over a BIACORE flow cell, where biotinylated α-bgt had previously been captured by streptavidin.

Regarding peptides shortened at the N terminus, the 13-mer peptide showed a sharp drop in binding, whereas peptides lacking both H_1 and R_2 positions did not bind α-bgt (Figure 2A). When peptides shortened at the C terminus were studied, it was found that those shorter than 11-mer did not bind α-bgt (Figure 2B). The minimal essential binding sequence was therefore R_2YYESSLEPW$_{11}$, which is in good agreement with results obtained by structure-based comparison of p6.7 with models of the nicotinic receptor binding sites (Table 1).

Systematic Affinity Maturation of the Peptide Mimotope

In an attempt to obtain an increase in α-bgt binding affinity with respect to the original p6.7 peptide, an iterative process was carried out. Structural analysis of p6.7 and progressive shortening of peptide sequence respectively indicated peptide sequences 3–10 and 2–11 as essential for binding. On this basis, positions 1, 12, 13, and 14 of the peptide sequence, one at a time, were systematically redefined, introducing each of the 19 L-amino acids (C was omitted to avoid thiol oxidation). Peptide binding to α-bgt was analyzed by BIACORE, and sequences were selected on the basis of their k_{off}. Ranking of peptide k_{off} by BIACORE is fast and can be done in a single run, using unlabeled crude peptide samples. It is therefore particularly suitable for sequence selection from peptide libraries.

Analysis of peptide-α-bgt binding showed that the 11-mer peptide with F in position 1 had the lowest k_{off} (1.05×10^{-3} s^{-1}), lower than the 11-mer peptide with H (like the original peptide p6.7) in this position. F was then selected in position one, and the iterative process was repeated to define position 12. Peptides with D or P in this position had the lowest k_{off}.

Since the selected F_1RYYESSLEPWD$_{12}$ and F_1RYYESSLEPWP$_{12}$ peptides were found to have similar k_{off} ($7 \times 10^{-4}s^{-1}$ and $8 \times 10^{-4}s^{-1}$, respectively) both were used to construct further 13-mer sublibraries. From the results of peptide k_{off} analysis of these sublibraries, peptides with D in position 13 were selected. The addition of another D in position 14 produced a further decrease in k_{off} ($2 \times 10^{-4}s^{-1}$) of the 13-mer peptide with D_{12} ($3.1 \times 10^{-4}s^{-1}$) (Figure 3).

Affinity maturation of the lead p6.7 peptide enabled new sequences, quite different from receptor native sequences, to be selected. Although Y_{12} corresponds to a highly conserved residue in α-bungarotoxin binding receptors, its replacement in the p6.7 sequence resulted in an increase in toxin binding. In peptides with the lowest k_{off}, Y_{12} is replaced by D or P, both having significant chemical differences from the aromatic residue of the native sequence. However, structural studies and empirical definition of p6.7 minimum binding sequence, both excluded Y_{12} from the main peptide interacting structure.

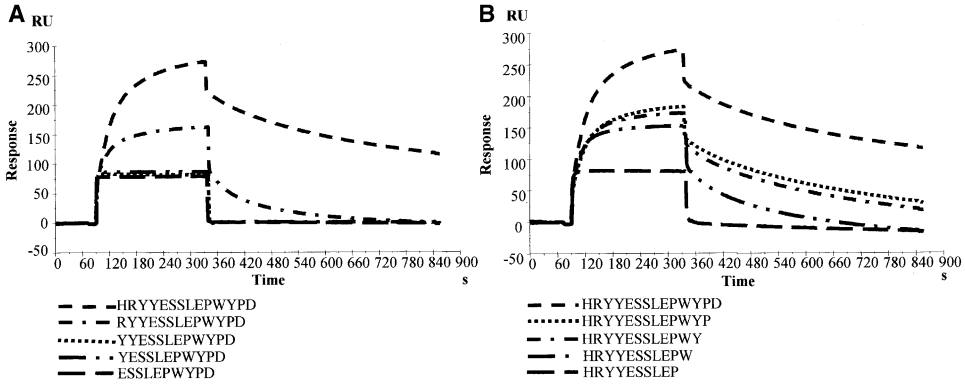

Figure 2. Definition of p6.7 Minimal α-bgt Binding Sequence

α-bgt binding of peptide from p6.7 sequence, progressively shortened at N- (A) and C (B) termini, was analyzed by BIACORE on α-bgt-biotin SA sensor chip. Peptide concentration was 10 μg/ml, flow rate 10 μl/min.

Association and dissociation kinetic rates (k_{on} and k_{off} respectively) and affinity constants (K_A) of the selected 13-mer and 14-mer peptides, having the sequences F_1RYYESSLEPWDD$_{13}$ (13-merDD) and F_1RYYESSLEPW DDD$_{14}$ (14-merDDD), respectively, were calculated from BIACORE sensorgrams obtained at different peptide concentrations, and compared with those of the original peptide mimotope p6.7. The 14-merDDD peptide had a K_A (1×10^8 M^{-1}) ten times that of the peptide p6.7, essentially determined by the 1 log decrease in the k_{off} (Figure 4).

IC_{50}

The half-maximal inhibition constant IC_{50} was calculated for 13-merDD and 14-merDDD peptides by a solid phase radioimmunoassay using ^{125}I-α-bgt and affinity-purified nAchR from *Torpedo* electric organs and was one tenth that of peptide p6.7, in line with their different affinities (Figure 5). The IC_{50} of the 14-merDDD peptide (2.5 nM) is analogous to the IC_{50} of the previously described HAPep [16].

In Vitro and In Vivo Activity of High-Affinity MAPs

The tetrameric p6.7 peptide proved to be an effective antidote against α-bgt at a dose of 100 μg/mouse. Although the monomeric peptide had the same K_A and IC_{50}, it was ineffective in vivo, even at a dose ten times that of the corresponding tetrameric peptide [17]. Selected 13-merDD and 14-merDDD peptides derived from affinity maturation of the lead p6.7 peptide, were then synthesized in a tetra-branched multiple antigen peptide (MAP) form and tested for their ability to inhibit α-bgt binding to nAchR, in vitro and in vivo.

We compared α-bgt binding capacity of MAPs with those of the respective monomeric peptides. As we observed in [17], tetrameric peptides retained the functional properties of the corresponding monomeric peptides in vitro, with nearly identical K_A and IC_{50}.

Kinetic rates and affinity of toxin binding sites of MAP peptides were calculated by immobilizing biotin-labeled tetra-branched peptide on a streptavidin-coated BIACORE SA sensor chip, using α-bgt as analyte in solution, in order to avoid multivalent binding [17]. The K_A results were 9.46×10^7 for MAP$_4$13-merDD and 1.9×10^8 for MAP$_4$14-merDDD. IC_{50}, calculated by competition RIA, results were 1.4×10^{-9} M for MAP$_4$13-merDD and 0.97×10^{-9} M for MAP$_4$14-merDDD.

We tested the ability of the selected tetrameric 13-merDD and 14-merDDD peptide to neutralize α-bgt lethality in vivo. To compare the in vivo activity of monomeric and tetrameric peptides, mice were injected subcutaneously with 10 μg of α-bgt, and after 5 min, they were given tetrameric or monomeric peptides. The tetrameric peptides were highly effective in neutralizing the lethality of the toxin, whereas the monomeric peptides were ineffective, even when used at five times the dose of the corresponding tetra-branched peptides.

Since the 13-merDD and 14-merDDD MAPs showed very similar protective activity against α-bgt toxicity when tested at different concentrations on a small popu-

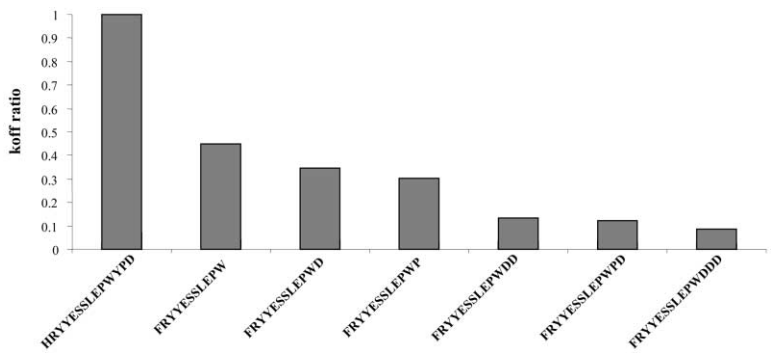

Figure 3. Affinity Maturation of p6.7

Peptides k_{off} ratio with respect to p6.7 is shown. Peptides diluted to 10 μg/ml were injected at 10 μl/min over α-bgt-biotin SA sensor chip; flow rate was 10 μl/min. Peptide k_{off} were calculated with BIAevaluation 3.0 software.

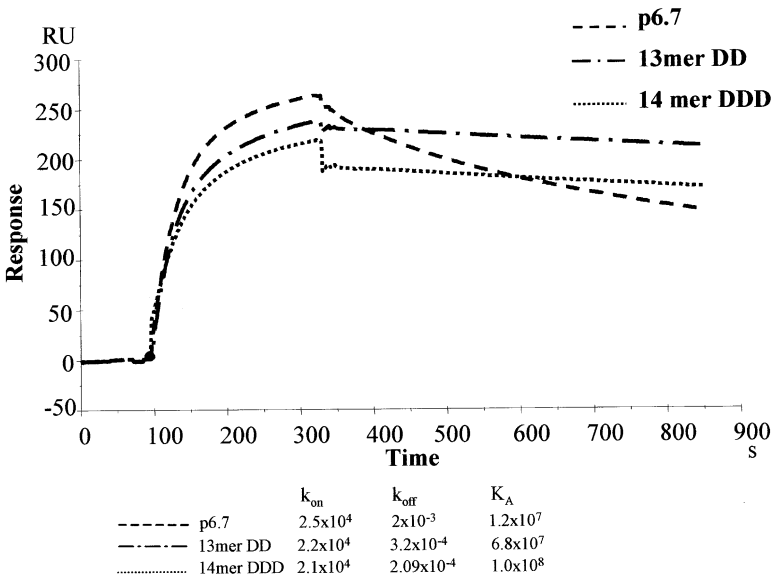

Figure 4. Comparison of α-bgt Binding of p6.7 and Selected 13-merDD and 14-merDDD Peptides

Peptides at concentrations ranging from 0.1 to 10 μg/ml were injected over α-bgt-biotin SA sensor chip. Flow rate was 10 μl/min. Kinetic rates and affinity constants were calculated by BIAevaluation 3.0 software. The overlay of sensorgrams obtained with 2 μg/ml is reported in the figure.

lation of animals, we chose to test only the 14-mer MAP, which seemed slightly more effective at low concentrations, on a larger population. The results are reported in Table 2. Using the 14-merDDD peptide, injection of 100 μg monomeric peptide did not protect mice from the effect of the toxin, since all died in about 1 hr. A dose of 5 μg MAP produced a 2.5–5 hr delay in the lethal effect, whereas a 10 μg sample of MAP protected 25% of the mice from toxin lethality. Five out of twenty mice injected with 10 μg MAP survived with no symptoms, seven mice died in 5–7 hr, seven died in about 24 hr, and one survived for 48 hr. Injection of 20 μg MAP completely neutralized α-bgt lethality in mice.

Despite the increase in affinity with respect to the lead peptide p6.7, neither the 13-merDD nor the 14-merDDD monomeric peptide induced protection against α-bgt lethality in mice, at a dose of 100 μg. This is in agreement with what already reported for HAPep, which having the same IC_{50} as the 14-merDDD conferred protection from α-bgt only at a dose of 5 mg per mouse [16]. A cyclic peptide, derived from the LLPep [15], and with a higher affinity than LLPep itself, although showing a higher IC_{50} (12 nM) with respect to HAPep, results were more effective in vivo (2.5 mg per mouse) [30]. Cyclization is a well-known strategy to confer in vivo stability to peptides, and this, more than an increase in affinity, might have been responsible for the increased in vivo efficiency of the cyclic peptide.

The in vivo efficiency of branched peptides with respect to the corresponding monomeric forms, was shown previously [17]. The increased in vivo activity of the here described high affinity MAPs with respect to the lead tetrameric p6.7 peptide reflects, indeed, the difference in affinity and IC_{50} of the new mimotope peptides.

This result opens new perspectives that go beyond use of our high-affinity peptide mimotopes as synthetic antidotes against snake neurotoxin.

Significance

Structural comparison of the complex of α-bgt with the peptide mimotope of the nicotinic receptor ligand binding site, p6.7, with available structural models for the nicotinic receptor neurotoxin binding site allowed defining of the putative critical interaction region of

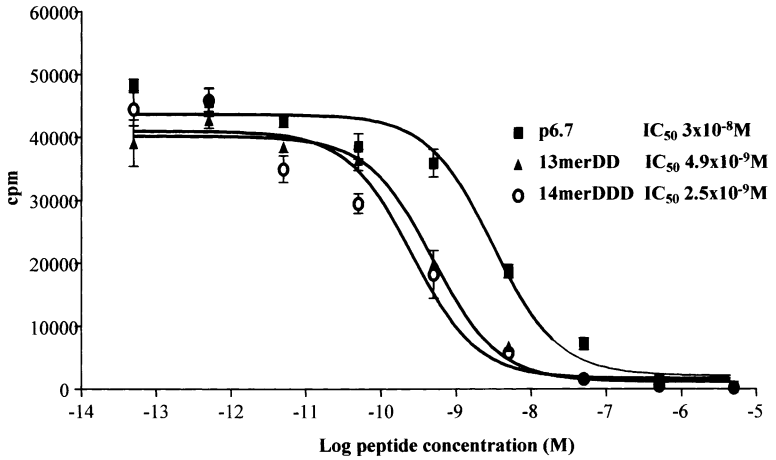

Figure 5. Inhibition of ^{125}I-α-bgt Binding to *Torpedo* nAchR by p6.7, 13-merDD, and 14-merDDD

Peptides at different concentrations, ranging from 5 μM to 50 fM, were incubated with 10^5 cpm of ^{125}I-α-bgt (Amersham Italia Srl) for 1 hr at room temperature on plates coated with affinity-purified nAchR. Assays were performed in triplicate and the half-maximal inhibition constant IC_{50} was calculated by nonlinear regression analysis using GraphPad Prism 3.02 software.

Table 2. In Vivo Activity of Monomeric and Tetrameric Peptides

	Amount (μg)[a]					
No. of Mice	α-bgt	Monomeric 13-merDD	MAP_4 13-merDD	Monomeric 14-merDDD	MAP_4 14-merDDD	Outcome[b]
14	10	-	-	0	0	14 dead after 28 ± 3[c] min
3	10	-	-	100	0	3 dead after 59 ± 3[c] min
11	10	-	-	0	5	11 dead after 220 ± 68[c] min
20	10	-	-	0	10	5 alive 7 dead after 389 ± 64[c] min 7 dead after 1291 ± 142[c] min 1 dead after 2880 min
12	10	-	-	0	20	12 alive
3	10	100	0	-	-	3 dead after 48 min ± 2[c]
3	10	0	5	-	-	3 dead after 50 min ± 10[c]
3	10	0	10	-	-	2 alive 1 dead after 180 min
5	10	0	20	-	-	5 alive

[a] Subcutaneous injection.
[b] Treated mice were followed for 10 days.
[c] Standard deviation.

the peptide. This information was confirmed experimentally by progressive deletion of peptide terminal residues, which enabled definition of the minimal essential binding sequence. On this basis, affinity maturation of the lead p6.7 peptide mimotope was obtained by randomization of residues flanking the minimal binding sequence and direct functional selection of new peptides according to k_{off}. A peptide mimotope that binds α-bgt with almost ten times the affinity of the lead peptide p6.7 was obtained. Moreover, the tetra-branched form of the resulting high-affinity peptide was effective as antidote in vivo at a significantly lower dose than the tetra-branched lead peptide. In conclusion, structural-based design combined with constructed molecular diversity and functional selection, made it possible to develop a specifically targeted peptide ligand of high affinity.

We recently demonstrated that some of the problems related to the low activity of synthetic peptides in vivo can be overcome by synthesis of branched peptides [17]. This result is confirmed in the present study, where the tetra-branched peptide bioactivity fully reflects the increase in affinity, whereas the monomeric peptide bioactivity does not. Branched peptides have a clear pharmacological advantage over linear monomeric peptides, an advantage unrelated to the possibility of multimeric binding, but probably to a different clearance and resistance to proteolysis. This can increase the in vivo therapeutic and diagnostic use of peptides specifically directed to soluble (like toxin from certain pathogens) and extracellular (like membrane tumor antigens) targets.

Experimental Procedures

Structural analyses and graphical representations were realized with MolMol Software [31].

Peptide Synthesis

Monomeric peptides were synthesized as peptide amides by an automated synthesizer (MultiSynTech, Witten, Germany) on a Rink Amide MBHA resin (Nova Biochem) using 9-fluorenylmethoxycarbonyl chemistry and O-(benzotriazol-1-yl)-N,N,N′,N′-tetramethyluronium hexafluorophosphate/1,3-diisopropylethylamine activation. MAPs were synthesized on $Fmoc_4$-Lys_2-Lys-βAla Wang resin.

Side chain protecting groups were tert-butyl ester for D and E; trityl for H, N, and Q; tert-butoxycarbonyl for K and W; 2,2,4,6,7-pentamethyldihydrobenzofuran-5-sulfonyl for R; and tert-butyl ether for S, T, and Y.

Peptides were then cleaved from the resin and deprotected by treatment with trifluoroacetic acid containing water and triisopropylsilane (95/2.5/2.5).

Crude peptides were purified by reversed-phase chromatography on a Vydac C18 column. Identity and purity of final products was confirmed by electrospray (ESI) or matrix-assisted laser desorption ionization (MALDI) mass spectrometry.

SPR Experiments

SPR measurements were performed on a BIACORE 1000 Upgraded (BIACORE AB, Uppsala, Sweden). Biotin-conjugated-α-bgt was immobilized on a streptavidin-coated SA-sensor chip. For dissociation kinetic rate ranking, peptides diluted to 10 μg/ml in HEPES buffer saline (HBS) (10 mM HEPES, 150 mM NaCl, 3.4 mM EDTA, 0.005% polysorbate 20, pH 7.4) were injected at a flow rate of 10 μl/min over α-bgt. To calculate k_{on}, k_{off}, and K_A, purified peptides, diluted in HBS at concentrations ranging from 0.1–10 μg/ml, were used. Alternatively, biotinylated monomeric or tetra-branched peptides were immobilized on a streptavidin-coated SA-sensor chip and α-bgt, diluted at different concentration in HBS, was injected at a flow rate of 10 μl/min over each peptide.

k_{on}, k_{off}, and K_A were calculated using the BIAevaluation 3.0 software.

Radioimmunoassay

RIA competition experiments were performed on microtiter plates (Falcon 3912; Becton Dickinson, Oxanan, CA) coated over night at 4°C with affinity purified nAchR from *Torpedo* electric organs [32] (5 μg/ml in 0.05 carbonate buffer [pH 9.6]) and then blocked with 3% BSA in phosphate buffer saline (PBS) (pH 7.4) for 1 hr at room temperature. Peptides at concentrations ranging from 5 μM to 50 fM were incubated with 10^5 cpm of ^{125}I-α-bgt (Amersham Italia Srl) for 1 hr at room temperature. After washing with PBS, α-bgt binding to nAchR was detected by a γ-counter.

The half-maximal inhibition constant IC_{50} of each peptide was evaluated by nonlinear regression analysis of curves using GraphPad Prism 3.02 software.

In Vivo Experiments

For these experiments, 15 g Swiss mice were inoculated subcutaneously (s.c.) with 10 μg α-bgt (SIGMA) in 100 μl PBS (pH 7.4), and

after 5 min they were inoculated s.c. with different amounts of monomeric or MAP peptides in 250 μl PBS (pH 7.4). Mice treated with peptide antidotes were followed for 10 days.

Acknowledgments

The authors thank Miss Serena Lorenzini for her assistance with peptide synthesis. This research was supported by grants from the Italian Ministero dell'Istruzione, Università e Ricerca, (MIUR-PRIN 2002), and the University of Siena (PAR).

Received: February 7, 2003
Revised: March 20, 2003
Accepted: April 7, 2003
Published: May 16, 2003

References

1. Cortese, R., Monaci, P., Luzzago, A., Santini, C., Bartoli, F., Cortes, I., Fortugno, P., Galfre, G., Nicosia, A., and Felici, F. (1996). Selection of biologically active peptides by phage display of random peptide libraries. Curr. Opin. Biotechnol. *7*, 616–621.
2. Hruby, V.J., Ahn, J.M., and Liao, S. (1997). Synthesis of oligopeptide and peptidomimetic libraries. Curr. Opin. Chem. Biol. *1*, 114–119.
3. Meloen, R.H., Puijk, W.C., and Slootstra, J.W. (2000). Mimotopes: realization of an unlikely concept. J. Mol. Recognit. *13*, 352–359.
4. Partidos, C.D., and Steward, M.W. (2002). Mimotopes of viral antigens and biologically important molecules as candidate vaccines and potential immunotherapeutics. Comb. Chem. High Throughput Screen. *5*, 15–27.
5. Olszewska, W., Partidos, C.D., and Steward, M.W. (2000). Anti-peptide antibody responses following intranasal immunization: effectiveness of mucosal adjuvants. Infect. Immun. *68*, 4923–4929.
6. Chen, X., Scala, G., Quinto, I., Liu, W., Chun, T.W., Justement, J.S., Cohen, O.J., vanCott, T.C., Iwanicki, M., Lewis, M.G., et al. (2001). Protection of rhesus macaques against disease progression from pathogenic SHIV-89.6PD by vaccination with phage-displayed HIV-1 epitopes. Nat. Med. *7*, 1225–1231.
7. Chirinos-Rojas, C.L., Steward, M.W., and Partidos, C.D. (1998). A peptidomimetic antagonist of TNF-alpha-mediated cytotoxicity identified from a phage-displayed random peptide library. J. Immunol. *161*, 5621–5626.
8. Chirinos-Rojas, C.L., Steward, M.W., and Partidos, C.D. (1997). Use of a solid-phase random peptide library to identify inhibitors of TNF-alpha mediated cytotoxicity in vitro. Cytokine *9*, 226–232.
9. Bracci, L., Lozzi, L., Lelli, B., Pini, A., and Neri, P. (2001). Mimotopes of the nicotinic receptor binding site selected by a combinatorial peptide library. Biochemistry *40*, 6611–6619.
10. Karlin, A. (2002). Emerging structure of the nicotinic acetylcholine receptors. Nat. Rev. Neurosci. *3*, 102–114.
11. Arias, H.R. (1997). Topology of ligand binding sites on the nicotinic acetylcholine receptor. Brain Res. Brain Res. Rev. *25*, 133–191.
12. Neumann, D., Barchan, D., Fridkin, M., and Fuchs, S. (1986). Analysis of ligand binding to the synthetic dodecapeptide 185–196 of the acetylcholine receptor alpha subunit. Proc. Natl. Acad. Sci. USA *83*, 9250–9253.
13. McLane, K.E., Wu, X.D., Schoepfer, R., Lindstrom, J.M., and Conti-Tronconi, B.M. (1991). Identification of sequence segments forming the alpha-bungarotoxin binding sites on two nicotinic acetylcholine receptor alpha subunits from the avian brain. J. Biol. Chem. *266*, 15230–15239.
14. Lentz, T.L. (1995). Differential binding of nicotine and alpha-bungarotoxin to residues 173–204 of the nicotinic acetylcholine receptor alpha 1 subunit. Biochemistry *34*, 1316–1322.
15. Balass, M., Katchalski-Katzir, E., and Fuchs, S. (1997). The alpha-bungarotoxin binding site on the nicotinic acetylcholine receptor: analysis using a phage-epitope library. Proc. Natl. Acad. Sci. USA *94*, 6054–6058.
16. Kasher, R., Balass, M., Scherf, T., Fridkin, M., Fuchs, S., and Katchalski-Katzir, E. (2001). Design and synthesis of peptides that bind alpha-bungarotoxin with high affinity. Chem. Biol. *8*, 147–155.
17. Bracci, L., Lozzi, L., Pini, A., Lelli, B., Falciani, C., Niccolai, N., Bernini, A., Spreafico, A., Soldani, P., and Neri, P. (2002). A branched peptide mimotope of the nicotinic receptor binding site is a potent synthetic antidote against the snake neurotoxin alpha-bungarotoxin. Biochemistry *41*, 10194–10199.
18. Scarselli, M., Spiga, O., Ciutti, A., Bernini, A., Bracci, L., Lelli, B., Lozzi, L., Calamandrei, D., Di Maro, D., Klein, S., et al. (2002). NMR structure of alpha-bungarotoxin free and bound to a mimotope of the nicotinic acetylcholine receptor. Biochemistry *41*, 1457–1463.
19. Scherf, T., Balass, M., Fuchs, S., Katchalski-Katzir, E., and Anglister, J. (1997). Three-dimensional solution structure of the complex of alpha-bungarotoxin with a library-derived peptide. Proc. Natl. Acad. Sci. USA *94*, 6059–6064.
20. Scherf, T., Kasher, R., Balass, M., Fridkin, M., Fuchs, S., and Katchalski-Katzir, E. (2001). A beta-hairpin structure in a 13-mer peptide that binds alpha-bungarotoxin with high affinity and neutralizes its toxicity. Proc. Natl. Acad. Sci. USA *98*, 6629–6634.
21. Harel, M., Kasher, R., Nicolas, A., Guss, J.M., Balass, M., Fridkin, M., Smit, A.B., Brejc, K., Sixma, T.K., Katchalski-Katzir, E., et al. (2001). The binding site of acetylcholine receptor as visualized in the X-ray structure of a complex between alpha-bungarotoxin and a mimotope peptide. Neuron *32*, 265–275.
22. Spiga, O., Bernini, A., Scarselli, M., Ciutti, A., Bracci, L., Lozzi, L., Lelli, B., Di Maro, D., Calamandrei, D., and Niccolai, N. (2002). Peptide-protein interactions studied by surface plasmon and nuclear magnetic resonances. FEBS Lett. *511*, 33–35.
23. Smit, A.B., Syed, N.I., Schaap, D., van Minnen, J., Klumperman, J., Kits, K.S., Lodder, H., van der Schors, R.C., van Elk, R., Sorgedrager, B., et al. (2001). A glia-derived acetylcholine-binding protein that modulates synaptic transmission. Nature *411*, 261–268.
24. Brejc, K., van Dijk, W.J., Klaassen, R.V., Schuurmans, M., van Der Oost, J., Smit, A.B., and Sixma, T.K. (2001). Crystal structure of an ACh-binding protein reveals the ligand-binding domain of nicotinic receptors. Nature *411*, 269–276.
25. Moise, L., Piserchio, A., Basus, V.J., and Hawrot, E. (2002). NMR structural analysis of alpha-bungarotoxin and its complex with the principal alpha-neurotoxin-binding sequence on the alpha 7 subunit of a neuronal nicotinic acetylcholine receptor. J. Biol. Chem. *277*, 12406–12417.
26. Samson, A., Scherf, T., Eisenstein, M., Chill, J., and Anglister, J. (2002). The mechanism for acetylcholine receptor inhibition by alpha-neurotoxins and species-specific resistance to alpha-bungarotoxin revealed by NMR. Neuron *35*, 319–332.
27. Dougherty, D.A. (1996). Cation-pi interactions in chemistry and biology: a new view of benzene, Phe, Tyr, and Trp. Science *271*, 163–168.
28. Zhong, W., Gallivan, J.P., Zhang, Y., Li, L., Lester, H.A., and Dougherty, D.A. (1998). From ab initio quantum mechanics to molecular neurobiology: a cation-pi binding site in the nicotinic receptor. Proc. Natl. Acad. Sci. USA *95*, 12088–12093.
29. Fruchart-Gaillard, C., Gilquin, B., Antil-Delbeke, S., Le Novere, N., Tamiya, T., Corringer, P.J., Changeux, J.P., Menez, A., and Servent, D. (2002). Experimentally based model of a complex between a snake toxin and the alpha 7 nicotinic receptor. Proc. Natl. Acad. Sci. USA *99*, 3216–3221.
30. Balass, M., Kalef, E., Fuchs, S., and Katchalski-Katzir, E. (2001). A cyclic peptide with high affinity to α-bungarotoxin protects mice from the lethal effect of the toxin. Toxicon *39*, 1045–1051.
31. Koradi, R., Billeter, M., and Wüthrich, K. (1996). MOLMOL: a program for display and analysis of macromolecular structures. J. Mol. Graph. *14*, 51–55.
32. Lindstrom, J., Einarson, B., and Tzartos, S. (1981). Production and assay of antibodies to acetylcholine receptors. Methods Enzymol. *74*, 432–460.